ULTRASOUND NEWS

August 2023

JUM Journal of Ultrasound in Medicine

aium

Editor-in-Chief: Richard G. Barr, MD, PhD, FAIUM, FSRU, FACR

Impact factor (2022): 2.3

Journal Citation Reports (Clarivate, 2023): 15/31 (Acoustics (Science)) 83/135 (Radiology, Nuclear Medicine & Medical Imaging (Science))

Online ISSN: 1550-9613

© American Institute of Ultrasound in Medicine

Articles

Original Article | Open Access

Inter- and Intra-Operator Variability of Regularized Backscatter Quantitative Ultrasound for the Characterization of Breast Masses

Inter- and Intra-Operator Variability of Regularized Backscatter Quantitative Ultrasound for the Characterization of Breast Masses

Ana K. Argueta-Lozano, MSc, Laura Castañeda-Martinez, MSc, Vivian Bass, MSc, Maria-Julieta Mateos, MSc, PhD, Jorge P. Castillo-López, MSc, M. Patricia Perez-Badillo, MD, Lesvia O. Aguilar-Cortazar, MD, Fanny Porras-Reyes, MD, M. Isabel Sollozo-Dupont, PhD, Fabian Torres-Robles, MSc, EngD, Jorge Márquez-Flores, PhD, Yolanda Villaseñor-Navarro, MD, Raul Esquivel-Sirvent, PhD, Ivan M. Rosado-Mendez, MSc, PhD

Supplemental material online at jultrasoundmed.org

Objectives—Here we report on the intra- and inter-operator variability of the backscatter coefficient (BSC) estimated with a new low-variance quantitative ultrasound (QUS) approach applied to breast lesions in vivo.

Methods—Radiofrequency (RF) echo signals were acquired from 29 BIRADS 4 and 5 breast lesions in 2 sequential cohorts following 2 imaging protocols: cohort 1) radial and antiradial views, and cohort 2) short- and long-axis views. Protocol 2 was implemented after retraining and discussion on how to improve reproducibility. Each patient was scanned by at least 2 of 3 radiologists; each performed 3 acquisitions with transducer and patient repositioning in between acquisitions. BSC was estimated using a low-variance QUS approach based on regularization. Intra- and inter-operator variability of the intra-lesion median BSC was evaluated with a multifactorial ANOVA test (P-values) and the intraclass correlation coefficient (ICC).

Results—Inter-operator variability was only significant in the first protocol ($P < .007$); $ICC_{inter} = .77$ (95% CI .71–.82), indicating good inter-operator agreement. In the second protocol, the inter-operator variability was not significant ($P > .05$) and agreement was excellent ($ICC_{inter} = .92$ [.89–.94]). In both protocols, the intra-operator variability was not significant.

Conclusions—Our findings demonstrate the need for standardizing image acquisition protocols for backscatter-based QUS to reduce inter-operator variability and ensure its successful translation to the characterization of suspicious breast masses.

Key Words—backscatter coefficient; breast cancer; inter-operator variability; intra-operator variability; quantitative ultrasound; regularization

Figure 2. B-mode images of lesion 25 acquired by (**A**) radiologist 1, (**B**) radiologist 2, and (**C**) radiologist 3, along with their corresponding backscatter coefficient parametric images, including definition of the 1-mm border around the lesion estimated from the acquisitions of (**D**) radiologist 1, (**E**) radiologist 2, and (**F**) radiologist 3.

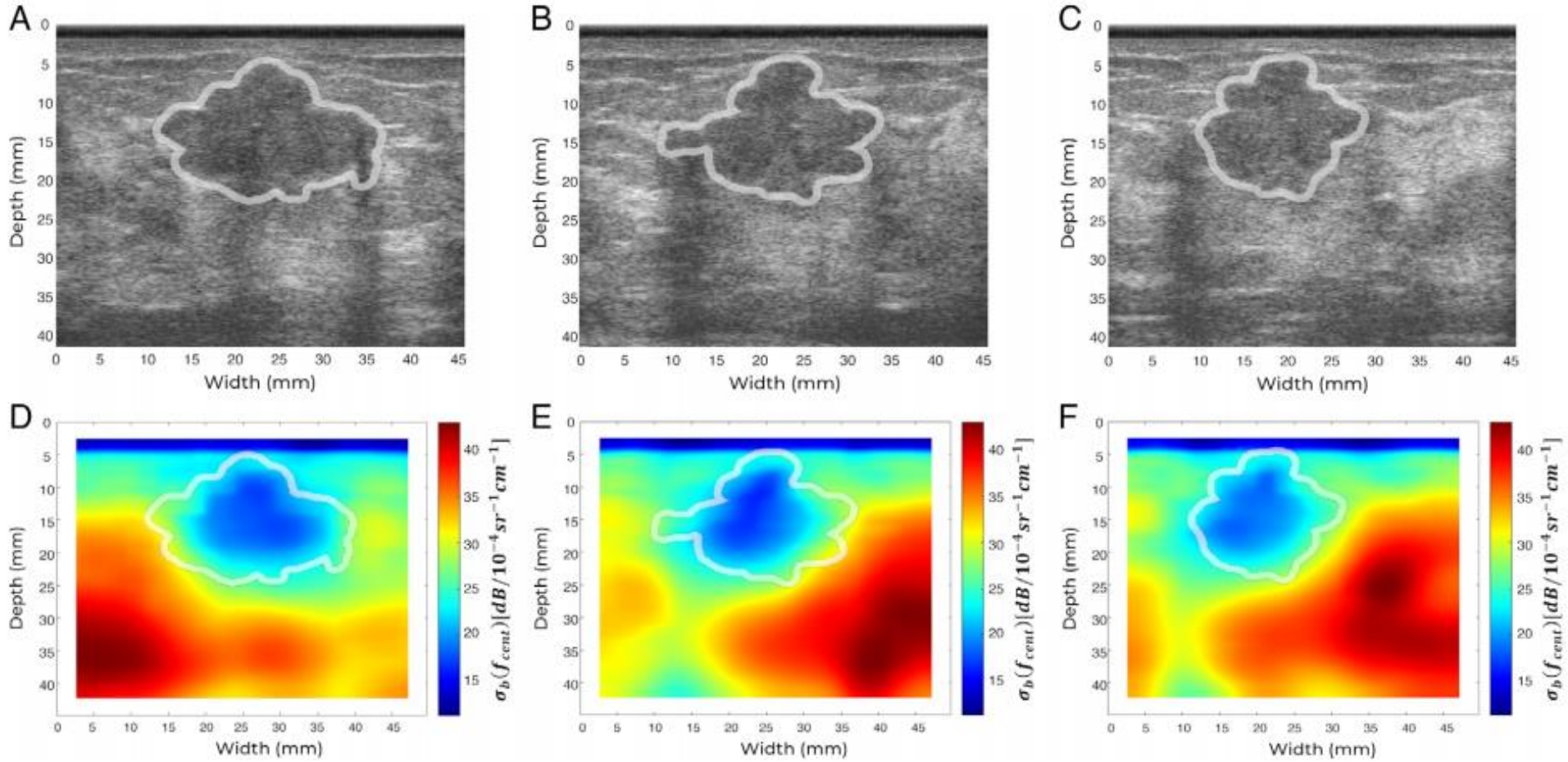

Figure 5. Left: B-mode image, right: parametric image of the backscatter coefficient at the center frequency for lesion 1. The different types of tissue surrounding the breast lesion are indicated: adipose tissue, fibroglandular tissue and the pectoral muscle. Red colors represent high values of $\sigma_b(f_{cent})$ and blue colors low values of $\sigma_b(f_{cent})$.

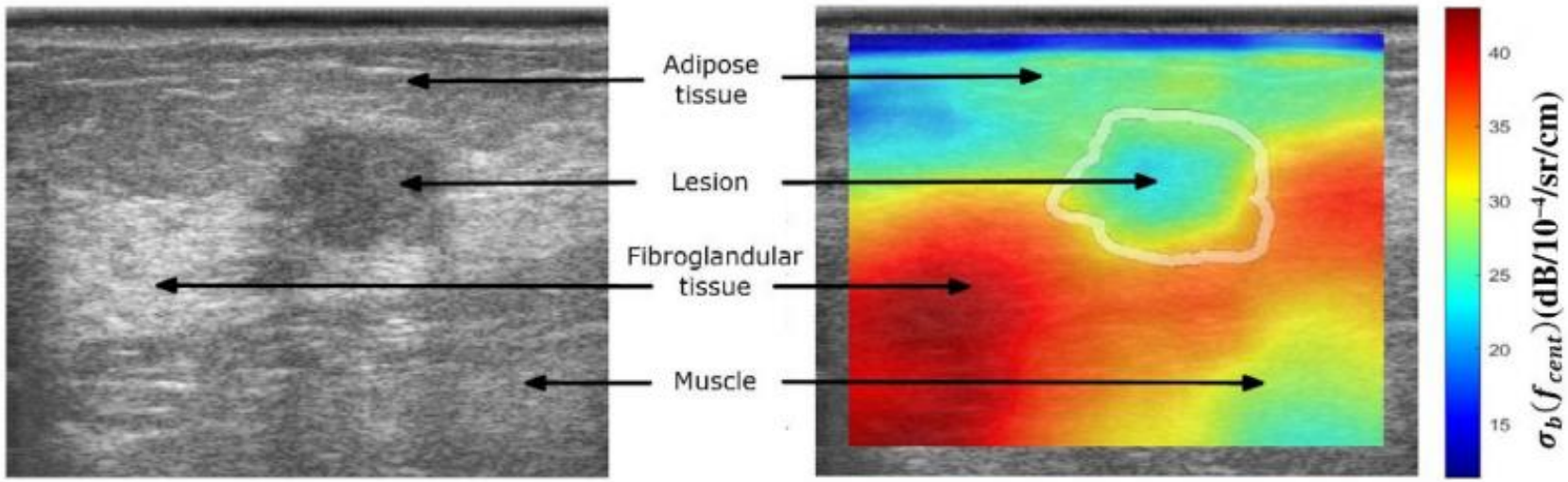

Visualizing the lymphatic vessels and flow with high-resolution ultrasonography and microvascular flow imaging

Joep J. J. Vullings[1], Caroline van Schaik[1], Jurgen J. Fütterer[1], Chris L. de Korte[2], Willemijn M. Klein[1]

[1]Department of Medical Imaging Radiology, Radboud University Medical Center, Nijmegen; [2]Department of Medical Imaging Radiology, Medical Ultrasound Imaging Center MUSIC, Radboud University Medical Center, Nijmegen, The Netherlands

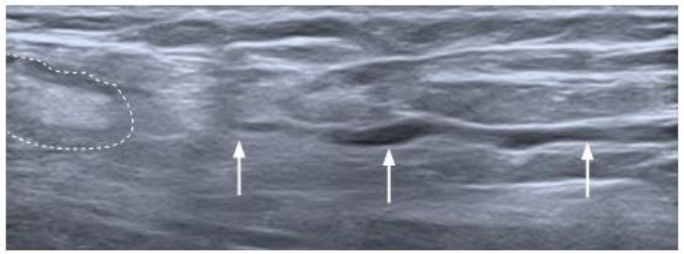

Fig. 4. **B-Mode image showing an inguinal lymph node with an afferent dilated lymphatic vessel.** Arrows show the afferent lymphatic vessel into an inguinal lymph node (dashed circle).

Imaging of the lymphatic system has always encountered difficulties, such as high costs, time-consuming procedures, and low-resolution images. Each method of imaging provides its own challenges. The use of high-resolution ultrasonography (HR-US) and microvascular flow imaging (MVFI) may prove to be the most effective method for visualizing the superficial lymphatic vessels. This study investigated the utilization of HR-US and MVFI in imaging inguinal lymph nodes and vessels, as well as the innovative use of an intranodal saline injection that acted as a contrast agent. This technical note aims to demonstrate that HR-US and MVFI, in combination with an intranodal saline injection, are applicable to the dynamic imaging of superficial inguinal lymph nodes and vessels.

Keywords: Ultrasonography; Lymphatic system; Lymphatic abnormalities; Lymphangiography

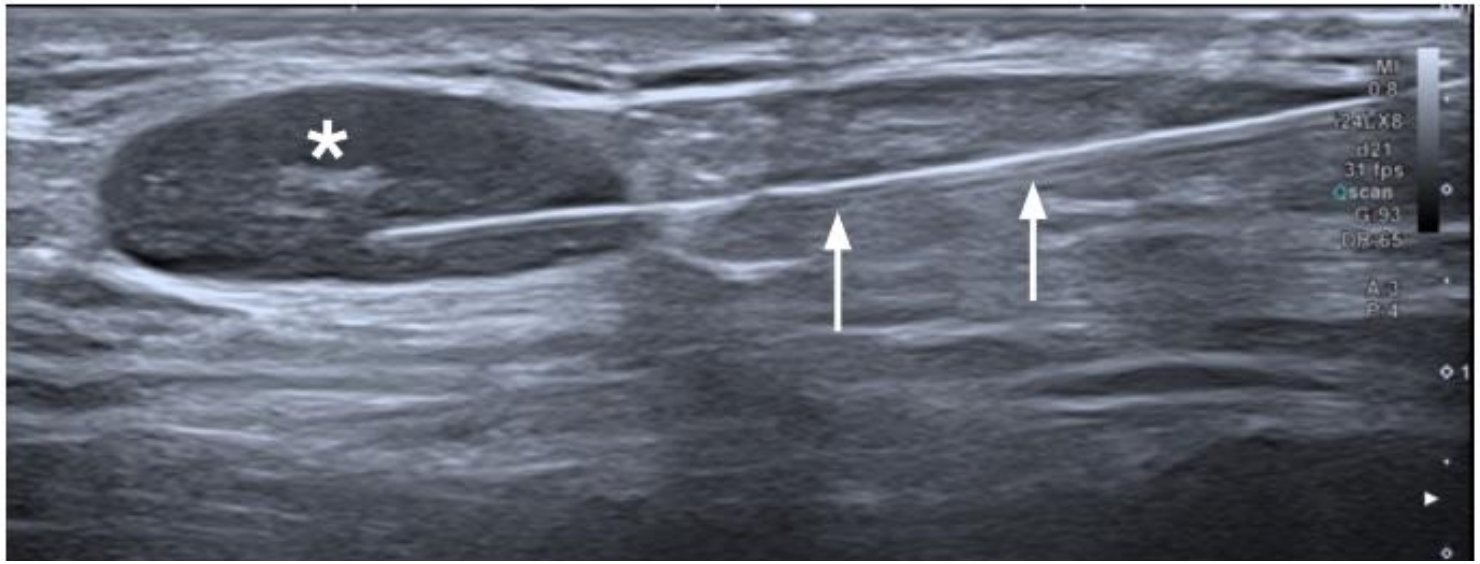

Fig. 1. **B-mode image showing normal inguinal lymph node (*) with 25G needle placed (arrows) at the corticomedullar border.**

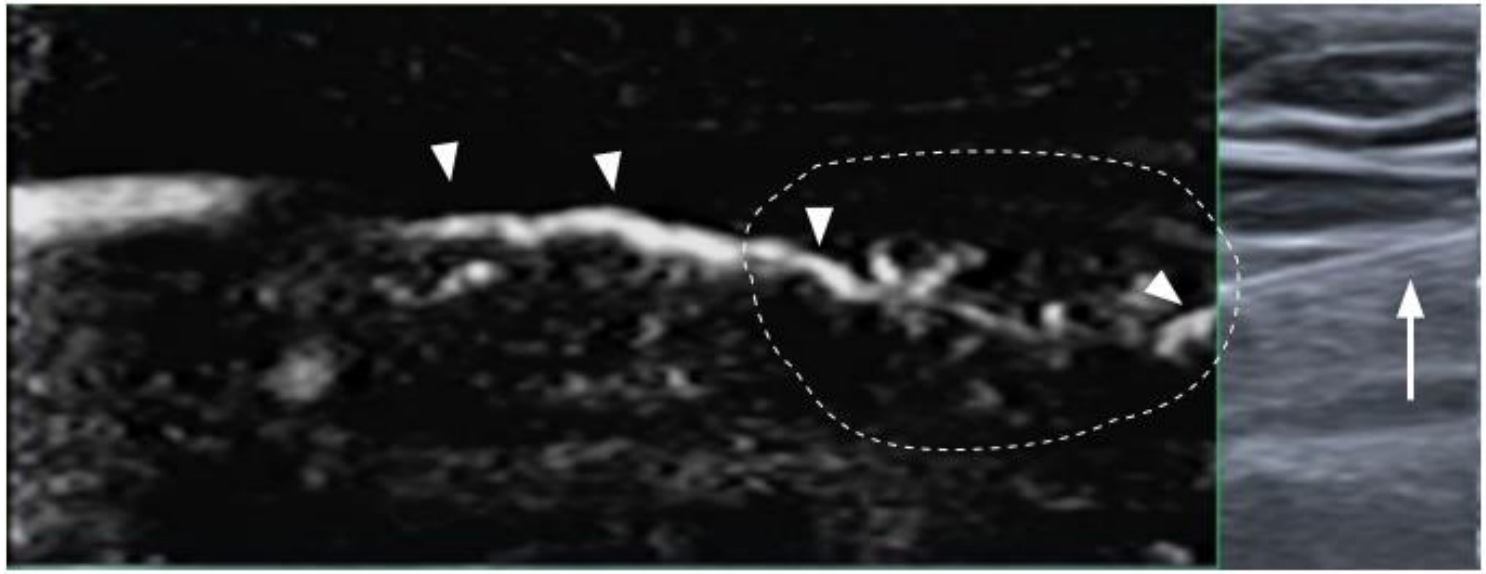

Fig. 2. **Superb Microvascular Imaging in an inguinal lymph node after saline injection.** The lymphatic cortex is depicted within the dashed circle with 25G needle (arrow) placed at the corticomedullar border. Antegrade lymph flow of the saline can be seen in the hilum and efferent lymph vessel (hyperechogenic depiction, annotated with arrowheads).

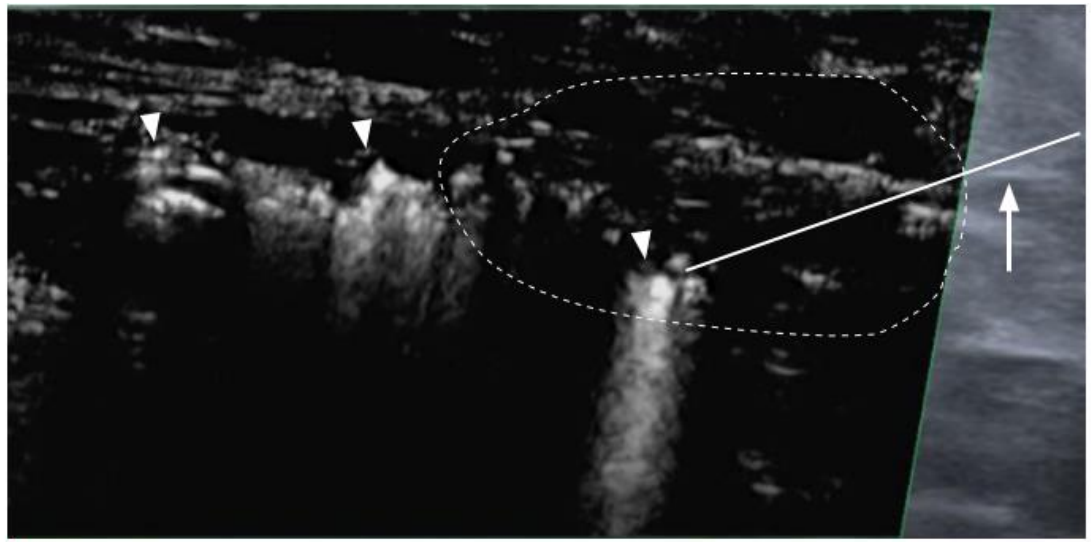

A

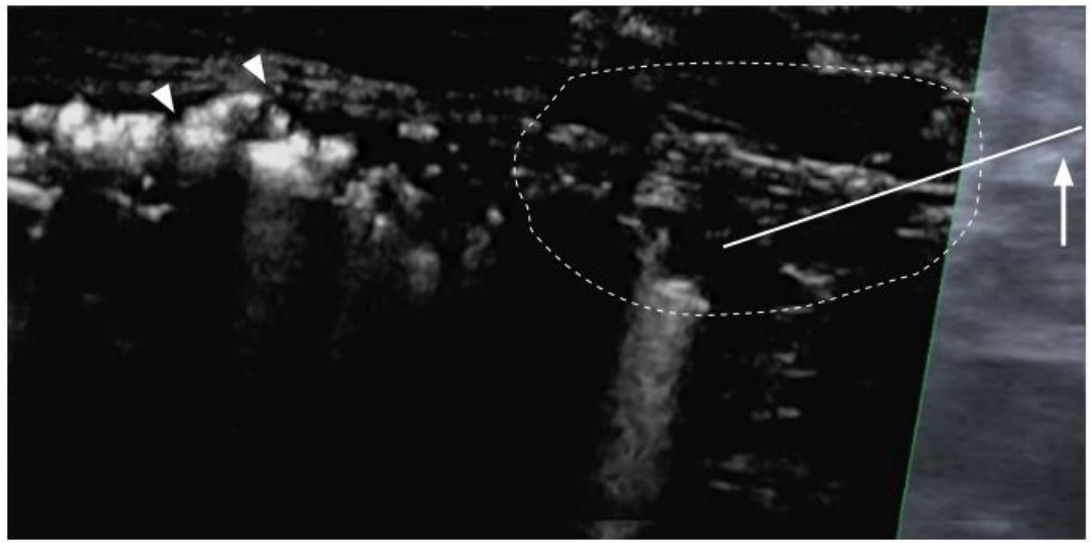

B

Fig. 3. **Superb Microvascular Imaging images of saline solution, injected with needle (arrow), at the corticomedullar border of an inguinal lymph node.**
A. Efferent lymph flow can be seen (arrowheads). B. Approximately 3 seconds after injection, tortuous lymph vessels were visible, just as dermal backflow started to occur and saline ventral effusion visualized (arrowheads). The lymphatic cortex is depicted with the dashed circle.

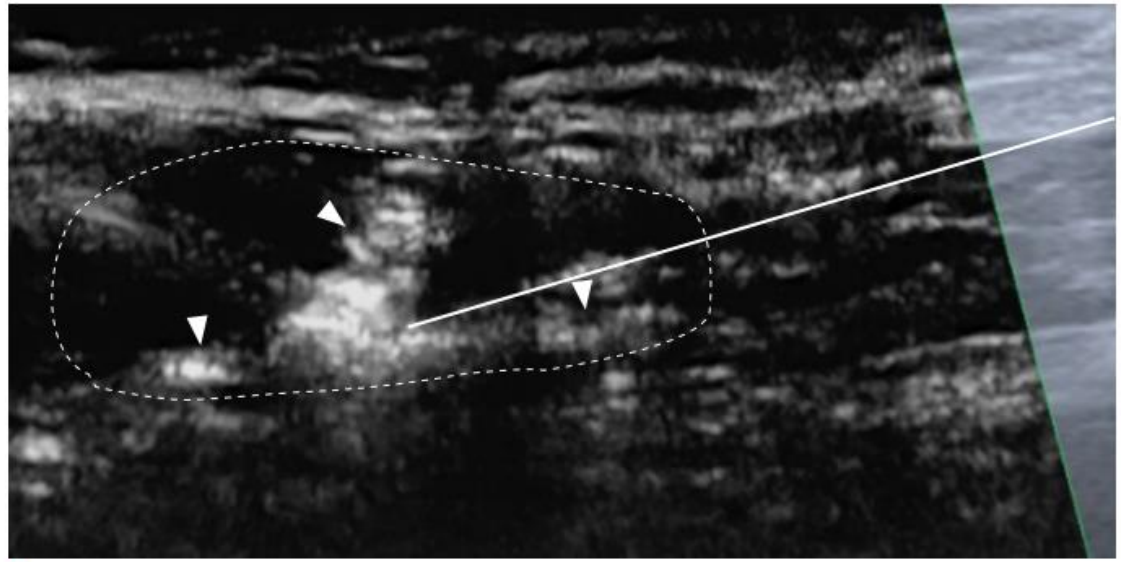

B

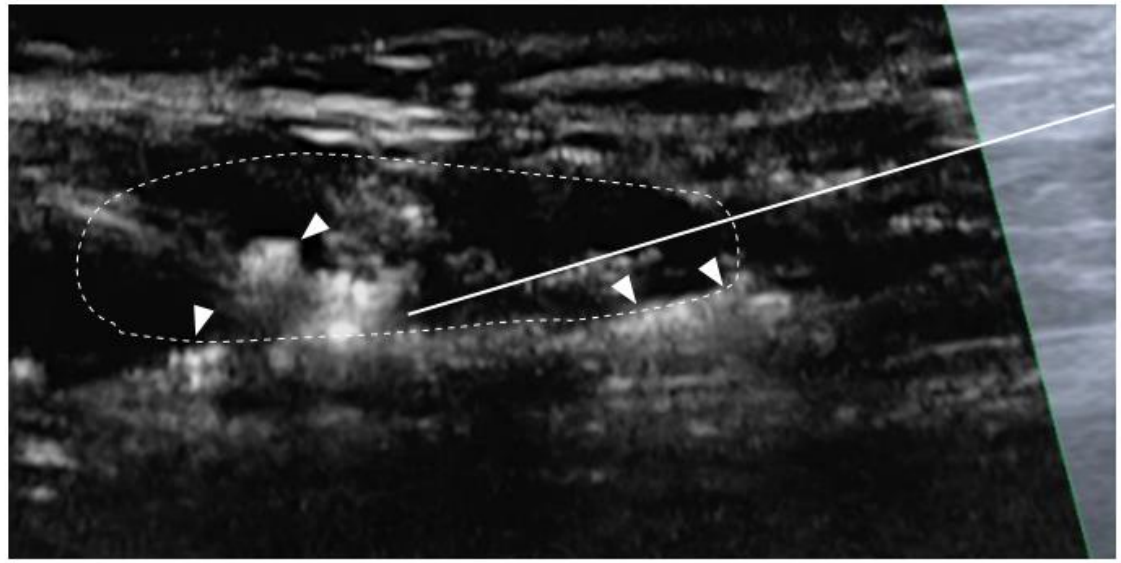

C

Fig. 5.Retrograde flow after saline injection.
A. Injection of saline solution into inguinal lymph node can be seen. Arrowheads indicate the flow from the injected saline solution at T=2.0 s post injection. B. Efferent lymph flow can be seen at T=0.4 s post injection, as well as retrograde flow, indicated by the right-sided arrowheads. C. Retrograde flow can be seen further upstream at T=0.7 s post injection. All arrowheads at the left side of the needle tip indicate efferent flow, all right-sided arrowheads indicate retrograde flow.

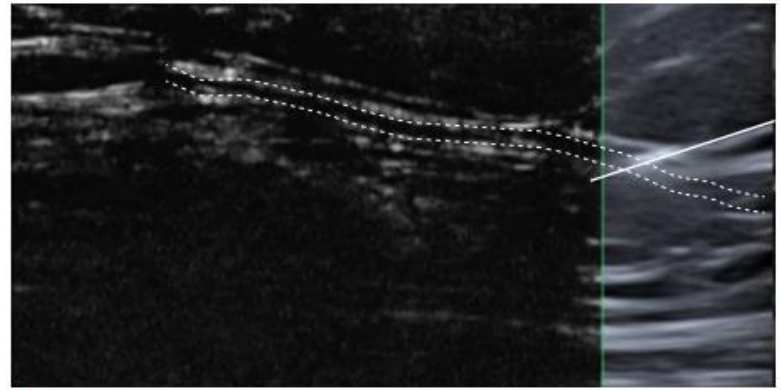

A

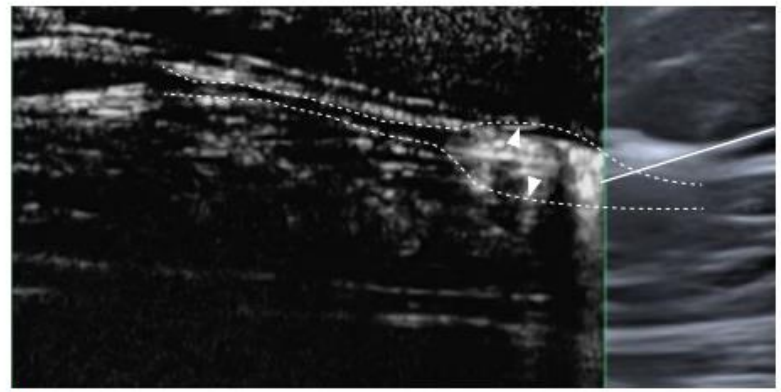

B

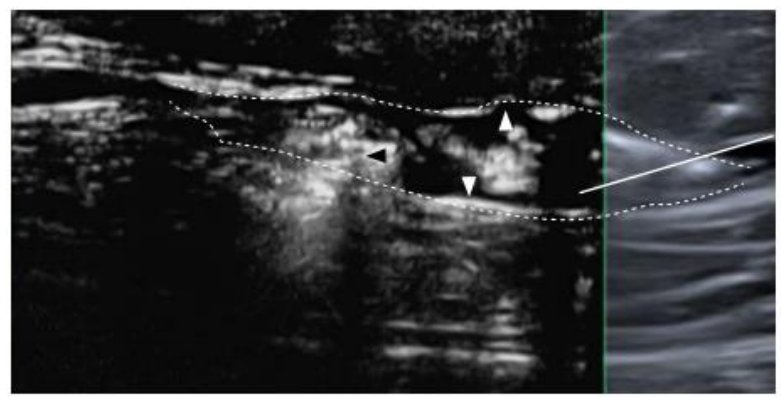

C

Fig. 6. Example of extravasation.
A. Needle was placed in a supposed lymph node. The dashed lines show the muscular fasciae. B. At T=1 s post injection, the injected saline (arrowheads) is visible. C. At T=4 s post injection the results of the extravasation show, when the saline pushes the fasciae apart (arrowheads).

The utility of two-dimensional shear wave elastography for predicting prostate cancer: a preliminary study

ULTRA SONO GRAPHY

Seong Soo Jeon[1], Chan Kyo Kim[2], Sung Yoon Park[2], Jae Hoon Chung[1], Minyong Kang[1], Hyun Hwan Sung[1], Byong Chang Jeong[1]

[1]Department of Urology, Samsung Medical Center, Sungkyunkwan University School of Medicine, Seoul; [2]Department of Radiology and Center for Imaging Science, Samsung Medical Center, Sungkyunkwan University School of Medicine, Seoul, Korea

ORIGINAL ARTICLE

https://doi.org/10.14366/usg.22202
eISSN: 2288-5943
Ultrasonography 2023;42:400-409

Purpose: This study investigated whether two-dimensional shear wave elastography (2D-SWE), using a newly developed device, is useful for predicting prostate cancer (PCa).

Methods: In this prospective study, 38 patients with suspected PCa underwent 2D-SWE, followed by a standard systematic 12-core biopsy with and without a targeted biopsy. Tissue stiffness on SWE was measured in the target lesion and in 12 regions of the systematic biopsies, and the maximum (E_{max}), mean (E_{mean}), and minimum (E_{min}) values of stiffness were generated. The area under the receiver operating characteristic curve (AUROC) for predicting clinically significant cancer (CSC) was calculated. Interobserver reliability and variability were evaluated using the intraclass correlation coefficient (ICC) and Bland-Altman plots, respectively.

Results: PCa was found in 78 of 488 regions (16%) in 17 patients. In region-based and patient-based analyses, the E_{max}, E_{mean}, and E_{min} values of PCa were significantly higher than those of benign prostate tissue ($P<0.001$). For the prediction of CSC, the AUROCs of E_{max}, E_{mean}, and E_{min} in the patient-based analysis were 0.865, 0.855, and 0.828, while that of prostate-specific antigen density was 0.749. In the region-based analysis, the AUROCs of E_{max}, E_{mean}, and E_{min} values were 0.772, 0.776, and 0.727, respectively. The interobserver reliability for the SWE parameters was moderate to good (ICC, 0.542 to 0.769), and the mean percentage differences on Bland-Altman plots were less than 7.0%.

Conclusion: The 2D-SWE method appears to be a reproducible and useful tool for the prediction of PCa. A larger study is warranted for further validation.

Received: December 7, 2022
Revised: February 4, 2023
Accepted: February 22, 2023

Correspondence to:
Chan Kyo Kim, MD, Department of Radiology and Center for Imaging Science, Samsung Medical Center, Sungkyunkwan University School of Medicine, 81 Irwon-ro, Gangnam-gu, Seoul 06351, Korea

Tel. +82-2-3410-0511
Fax. +82-2-3410-2559
E-mail: chankyokim@skku.edu

This is an Open Access article distributed under the terms of the Creative Commons Attribution Non-Commercial License (http://creativecommons.org/licenses/by-nc/4.0/) which permits unrestricted non-commercial use, distribution, and reproduction in any medium, provided the original work is properly cited.

Copyright © 2023 Korean Society of Ultrasound in Medicine (KSUM)

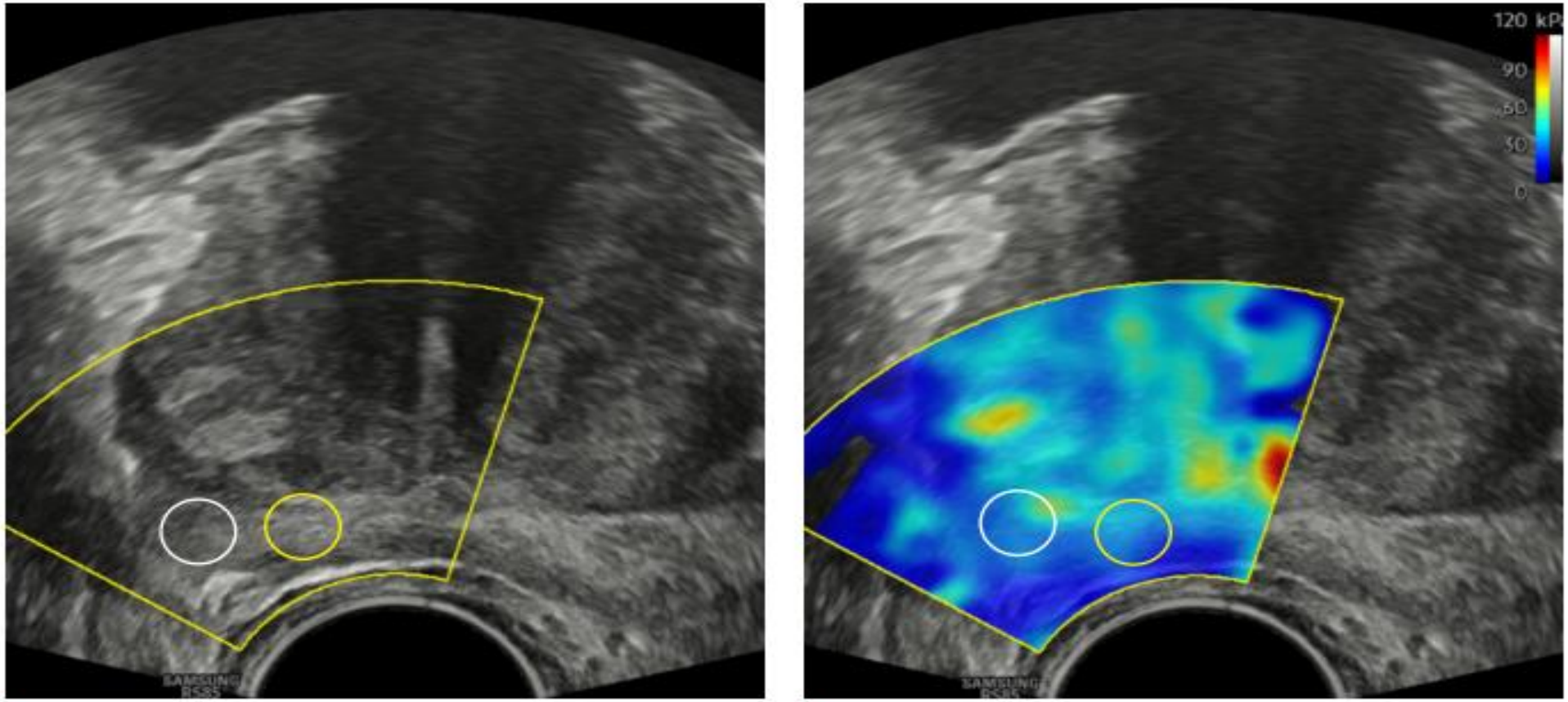

Fig. 1. Methods of acquisition for the 2D-SWE parameters.
2D-SWE images in a 61-year-old man show two 5-mm regions of interest on axial grayscale ultrasonography (A) and SWE (B) images, placed along the estimated path of the core biopsy in the right peripheral zone of the mid-gland. 2D-SWE, two-dimensional shear wave elastography.

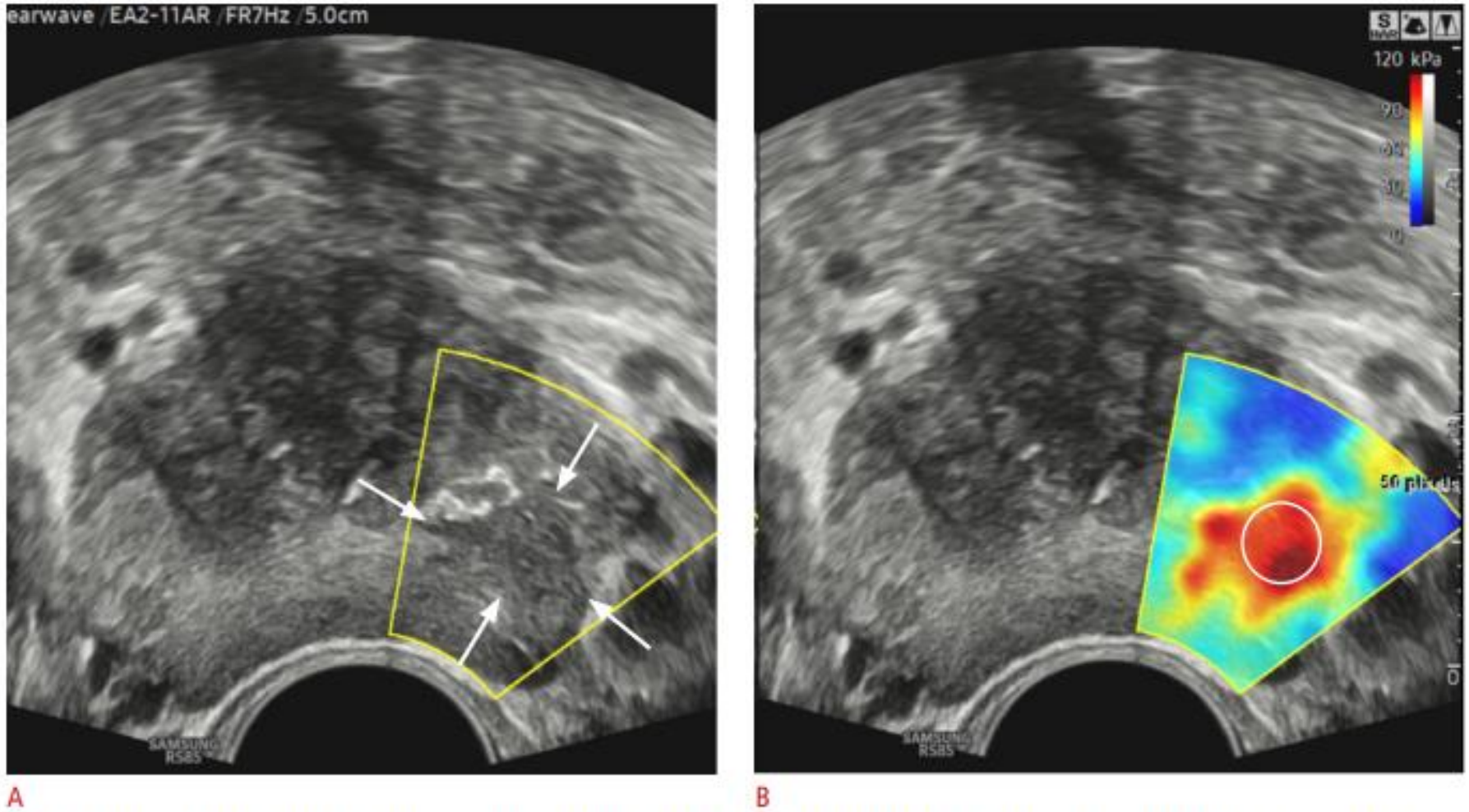

A B

Fig. 2. A 66-year-old man with prostate cancer in the left peripheral zone of the mid-gland (PSA=36.58 ng/mL, Gleason score 4+4).
A. Axial grayscale ultrasonography shows a focal hypoechoic lesion (arrows) in the left peripheral zone of the mid-gland, compared with the right peripheral zone. B. Axial 2D-SWE image shows increased stiffness in red (region of interest) in the corresponding site with A. The E_{max}, E_{mean}, and E_{min} values of PCa were 119.5, 111.7, and 88.3 kPa, respectively. PSA, prostate-specific antigen; 2D-SWE, two-dimensional shear wave elastography; E_{max}, maximum Young's modulus; E_{mean}, mean Young's modulus; E_{min}, minimum Young's modulus; PCa, prostate cancer.

Renal Doppler ultrasonography for predicting non-diabetic kidney disease in patients with diabetes

Sung Il Jung[1], Min Hoan Moon[2], Chang Kyu Sung[2], Myoung Seok Lee[2], Jeong Hwan Park[3], Sohee Oh[4]

[1]Department of Radiology, Konkuk University Medical Center, Research Institute of Medical Science, Konkuk University School of Medicine, Seoul; [2]Department of Radiology, [3]Department of Pathology, [4]Department of Biostatistics, Seoul Metropolitan Government Seoul National University (SMG-SNU) Boramae Medical Center, Seoul National University College of Medicine, Seoul, Korea

Purpose: This study was conducted to assess the role of renal Doppler ultrasonography (US) in predicting non-diabetic kidney disease (NDKD) in patients with diabetes, using histologic findings as the reference standard.

Methods: Fifty-nine consecutive patients with diabetes who underwent renal Doppler US and native kidney biopsy were included in this retrospective, single-institutional study. Based on histologic findings, patients were classified as having diabetic nephropathy (DN) or NDKD. Renal Doppler US findings, including cortical echogenicity, corticomedullary differentiation, and the resistive index (RI), were compared between DN and NDKD. A subgroup analysis according to chronic kidney disease (CKD) status was also performed.

Results: Cortical echogenicity and corticomedullary differentiation showed no significant differences between DN and NDKD (P=0.887 and P>0.99, respectively), whereas the RI was significantly higher in patients with DN than in those with NDKD (P=0.032). The subgroup analysis revealed a significant difference in the RI between DN and NDKD in patients with diabetes and CKD (P=0.010), but a significant difference was not found in those without CKD (P=0.713). When limited to patients with diabetes and CKD, the RI had an area under the curve value of 0.759, sensitivity of 57.1%, specificity of 81.0%, positive likelihood ratio of 3.0, and negative LR of 0.5 for predicting NDKD, using a cutoff value of ≤0.69.

Conclusion: Renal Doppler US may be useful in predicting NDKD in patients with diabetes and CKD.

Keywords: Diabetes mellitus; Non-diabetic renal disease; Renal Doppler ultrasonography; Kidney biopsy

ULTRA SONO GRAPHY

ORIGINAL ARTICLE

https://doi.org/10.14366/usg.23028
eISSN: 2288-5943
Ultrasonography 2023;42:440-445

Received: February 24, 2023
Revised: April 17, 2023
Accepted: May 12, 2023

Correspondence to:
Min Hoan Moon, MD, Department of Radiology, Seoul Metropolitan Government Seoul National University (SMG-SNU) Boramae Medical Center, Seoul National University College of Medicine, 20 Boramae-ro 5-gil, Dongjak-gu, Seoul 07061, Korea
Tel. +82-2-870-2531
Fax. +82-2-870-3539
E-mail: mmhoan@gmail.com

This is an Open Access article distributed under the terms of the Creative Commons Attribution Non-Commercial License (http://creativecommons.org/licenses/by-nc/4.0/) which permits unrestricted non-commercial use, distribution, and reproduction in any medium, provided the original work is properly cited.

Copyright © 2023 Korean Society of Ultrasound in Medicine (KSUM)

In conclusion, patients with diabetes who present with signs or symptoms of kidney disease may have NDKD and should be evaluated accordingly. Based on the high prevalence of NDKD in patients with diabetes and CKD who had **normal RIs**, a **normal intrarenal RI** may be a potential indicator for predicting NDKD in these patients. The authors hope that these findings will be helpful in managing patients with diabetes and CKD.

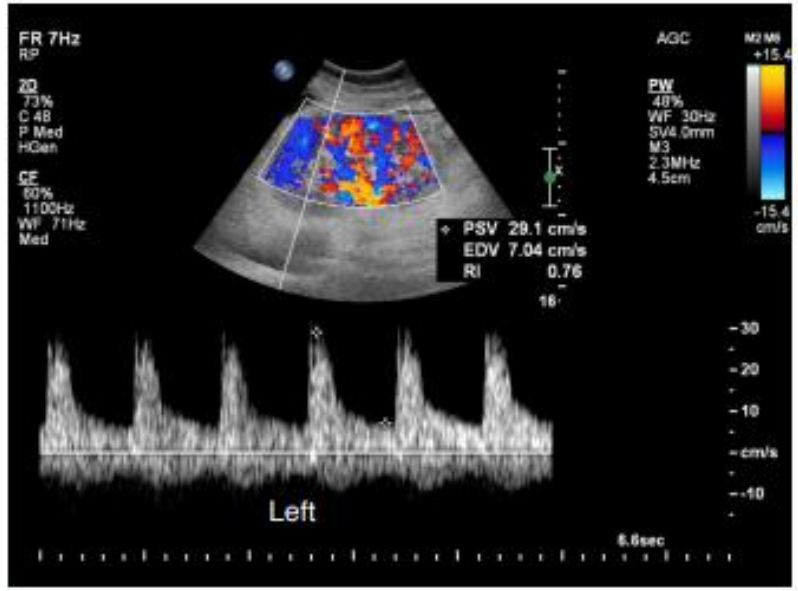

A

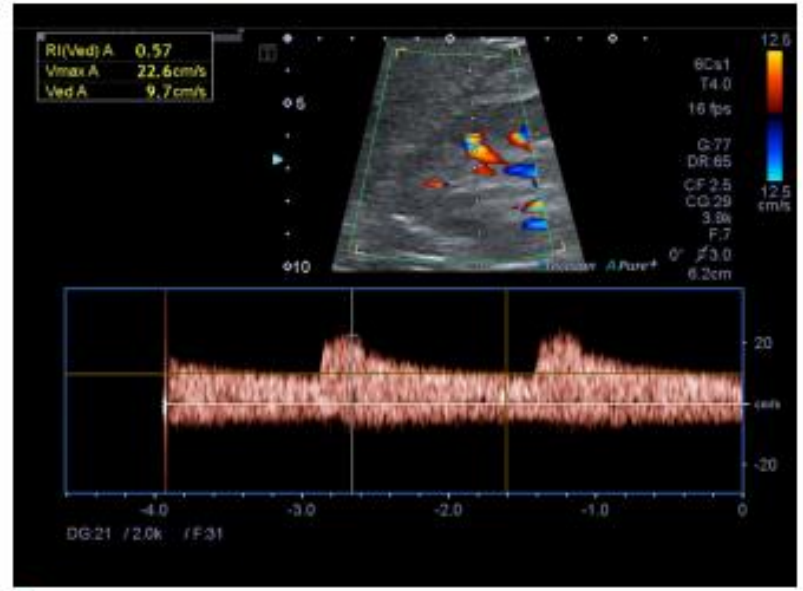

B

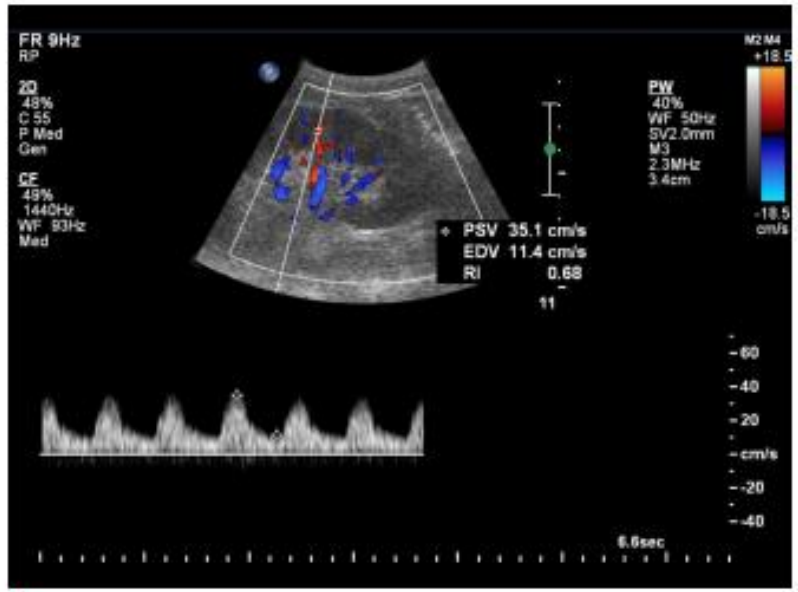

C

Fig. 2. **Renal Doppler US of patients with diabetes and CKD.**
A. A 42-year-old man with biopsy-proven DN shows an increased RI of 0.76. B. A 54-year-old man with biopsy-proven MPGN shows a normal RI of 0.57. C. A 62-year-old man with biopsy-proven MCD superimposed on DN shows a normal RI of 0.68. US, ultrasonography; CKD, chronic kidney disease; DN, diabetic nephropathy; RI, resistive index; MPGN, membranoproliferative glomerulonephritis; MCD, minimal change disease; PSV, peak systolic velocity; EDV, end-diastolic velocity.

RESEARCH ARTICLE

Assessment of portal system hemodynamics for the prediction of portal vein thrombosis in cirrhosis—A systematic review and meta-analysis

Suprabhat Giri MD, DM, Ankita Singh DNB, DM, Kailash Kolhe MD, DM, Marko Kozyk MBBS, Akash Roy MD, DM

First Published: 17 July 2023

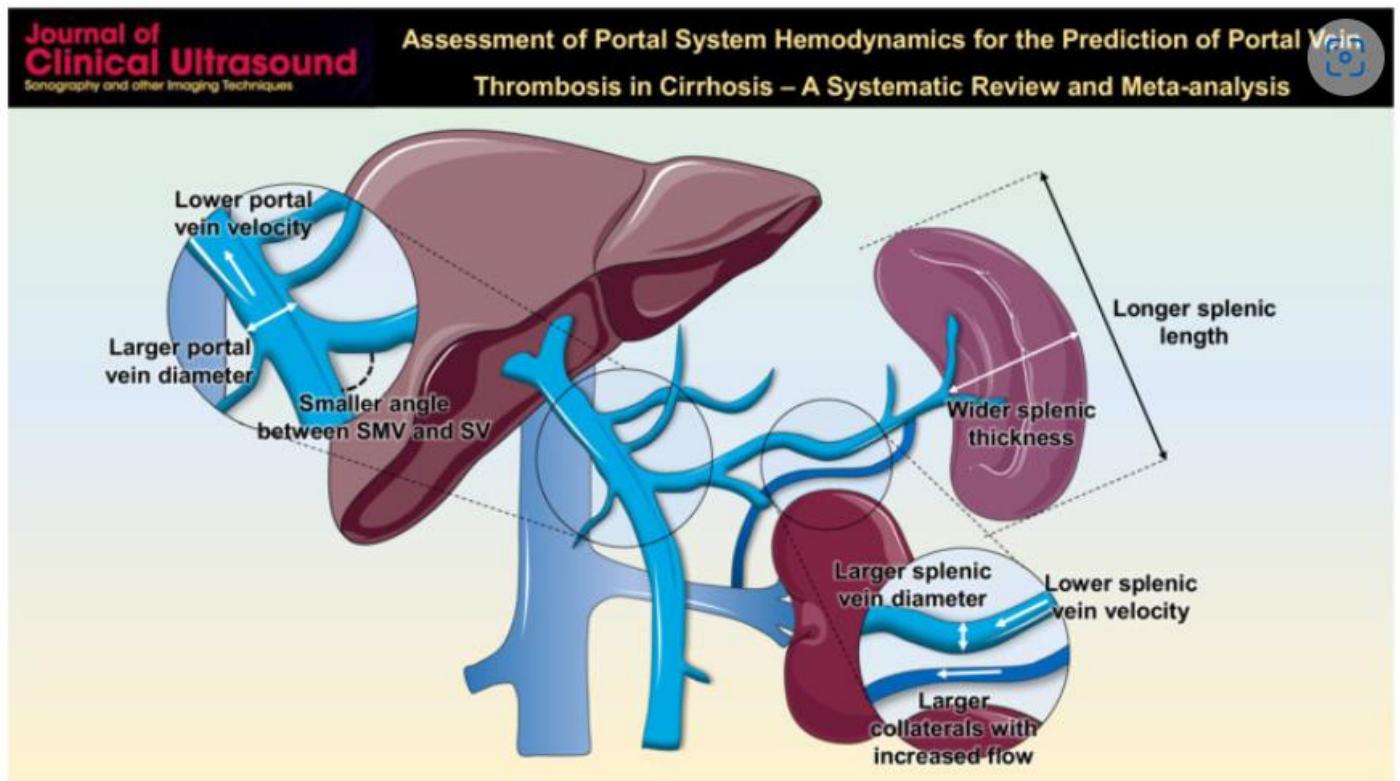

The assessment of portal hemodynamic parameters at baseline evaluation in cirrhotics may predict the development of portal vein thrombosis (PVT). A larger portal vein diameter, lower portal vein velocity, and a higher splenic length, thickness, and splenic vein velocity were significant predictors of PVT in cirrhotics without or with splenectomy.

CASE REPORT | Open Access

Isolated adductor longus avulsion in a young semi-professional football player: Imaging contribution and therapeutic considerations

Michele Abate, Luigi Sammarchi, Roberto Calà, Giacomo Milesi, Carmine Stefano Poerio, Riccardo Del Vescovo, Antonio Corvino, Andrea Delli Pizzi, Giulio Cocco, Vincenzo Salini

First Published: 19 July 2023

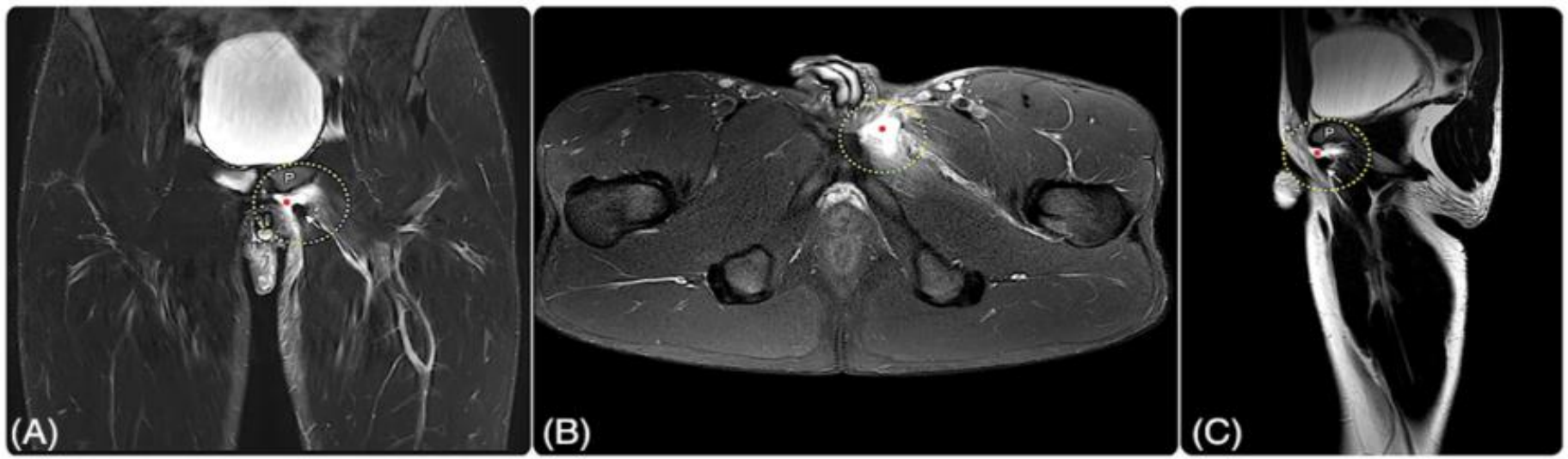

We reported a case of isolated adductor longus avulsion occurred in a young semi-professional football player. This article highlights the successful conservative treatment of an adductor longus avulsion with retraction and emphasizes the importance of regular clinical, instrumental, and objective assessments to facilitate a safe return to full athletic activity.